

Measurements of proton induced reaction cross sections on ^{120}Te for the astrophysical p -process

R. T. Güray*, N. Özkan, and C. Yalçın

Kocaeli University, Department of Physics, Umuttepe 41380, Kocaeli, Turkey

A. Palumbo, R. deBoer, J. Görres, P. J. LeBlanc, S.
O'Brien, E. Strandberg, W. P. Tan, and M. Wiescher

*University of Notre Dame, Department of Physics,
Notre Dame, Indiana 46556, USA*

Zs. Fülöp and E. Somorjai

ATOMKI, H-4001 Debrecen, POB.51., Hungary

H. Y. Lee and J. P. Greene

Argonne National Laboratory, Illinois 60439, USA

(Dated: October 19, 2018)

Abstract

The total cross sections for the $^{120}\text{Te}(p,\gamma)^{121}\text{I}$ and $^{120}\text{Te}(p,n)^{120}\text{I}$ reactions have been measured by the activation method in the effective center-of-mass energies $2.47 \text{ MeV} \leq E_{\text{c.m.}}^{\text{eff}} \leq 7.93 \text{ MeV}$ and $6.44 \text{ MeV} \leq E_{\text{c.m.}}^{\text{eff}} \leq 7.93 \text{ MeV}$, respectively. The targets were prepared by evaporation of 99.4% isotopically enriched ^{120}Te on Aluminum and Carbon backing foils, and bombarded with proton beams provided by the FN tandem accelerator at the University of Notre Dame. The cross sections and S factors were deduced from the observed γ ray activity, which was detected off-line by two Clover HPGe detectors mounted in close geometry. The results are presented and compared with the predictions of statistical model calculations using the codes NON-SMOKER and TALYS.

PACS numbers: 25.40.Lw, 26.30.-k, 27.60.+j

* Corresponding Author : tguray@kocaeli.edu.tr

I. INTRODUCTION

The elements heavier than iron ($Z > 26$) are mainly synthesized by three mechanisms: the s -process, r -process, and p -process, the latter being the least known among them. The p -process, responsible for the production of 35 proton-rich stable isotopes, can proceed via a combination of photodisintegration reactions $-(\gamma, n)$, (γ, p) and (γ, α) - on existing heavy s - and r -seeds in the temperature range of 2 - 3 x 10⁹ K. These high temperatures can be achieved in explosive environments, such as the O/Ne layers of Type-II supernovae [1, 2]. Initially, the nuclides are driven by a sequence of (γ, n) reactions to the proton-rich side of the valley of stability, whereby the binding energies of neutrons gradually increase along the isotopic path. When the (γ, p) and/or (γ, α) reaction rates become significant compared to those of the (γ, n) , the reaction path branches towards lower Z nuclei. While the photodisintegration reactions govern the overall reaction flow, complementary processes such as β^+ decays, electron captures, and (n, γ) reactions may play an important role as well. Recent p -process simulations demonstrate that (γ, α) reactions determine the overall reaction flow in between closed shells and affect the medium and heavy p -nuclei abundances. On the other hand, (γ, p) reactions provide important links for feeding p -process nuclei [3]. In particular, ¹²⁰Te is populated by a sequence of two photodisintegration reactions ¹²²Xe(γ, p)¹²¹I(γ, p)¹²⁰Te. Simulations indicate that ¹²⁰Te is underproduced in comparison to p -process abundance observations [3] which supports the results of earlier calculations [4, 5].

These p -process simulations rely on complex network calculations including more than 20000 reactions on about 2000 mostly unstable nuclei. Most of the reaction rates involved in these simulations are based on statistical model or Hauser-Feshbach predictions. The overall reliability of Hauser-Feshbach predictions in p -process simulations has been discussed [5]. Variations can lead to substantial changes in p -process abundance predictions. There is considerable effort to experimentally test the reliability of p -process predictions on selected cases [6, 7, 8, 9, 10, 11, 12, 13, 14, 15, 16, 17, 18, 19, 20, 21, 22, 23, 24, 25]. Since the photodisintegration process ¹²¹I(γ, p) directly feeds ¹²⁰Te, this reaction provides an excellent case for testing the reliability of the Hauser-Feshbach prediction near the closed proton shell $Z=50$; ¹²¹I has a high level density near the proton threshold and the reaction should be eligible for the statistical model prediction [26].

A direct measurement of the γ -induced photodisintegration $^{121}\text{I}(\gamma, p)^{120}\text{Te}$ is difficult since it requires photodisintegration of a short-lived radioactive ^{121}I isotopes. Direct (γ, p) and (γ, α) photodisintegration measurements have been demonstrated successfully [27, 28, 29] and p -process reactions with Coulomb dissociation techniques will be pursued at future radioactive beam facilities.

Presently the applicability of the statistical model approach is limited to testing the inverse radiative capture reaction process. A measurement of the radiative capture $^{120}\text{Te}(p, \gamma)^{121}\text{I}$ and the nuclear $^{120}\text{Te}(p, n)^{120}\text{I}$ reactions does not provide complete information about the reverse photodisintegration process but it is suitable for testing the reliability of the Hauser-Feshbach predictions [30] for these reaction channels. On the basis of the resulting statistical model parameters, the cross section predictions for the photodisintegration process can be directly deduced in the framework of the Hauser-Feshbach model [31].

The last decade has seen an increased interest in measuring the proton capture cross sections of p -nuclei [10, 11, 12, 13, 14, 15, 16, 17, 18, 19, 20, 21, 22, 23, 24, 25]. The bulk of these (p, γ) measurements have been done in the lower mass region ($A < 100$). The cross sections determined in these (p, γ) measurements generally agree with the statistical model predictions within a factor of two. In contrast, very few (p, n) measurements have been performed, again mainly on nuclei in the lower mass range of the p -process such as ^{76}Ge [10], ^{82}Se [11], and ^{85}Rb [24]. Measurements on ^{120}Te expand the range of p -process studies and address a case where the feeding process $^{121}\text{I}(\gamma, p)^{120}\text{Te}$ of a p -nucleus can be studied.

The charged-particle reaction cross sections for $^{120}\text{Te}(p, \gamma)^{121}\text{I}$ and $^{120}\text{Te}(p, n)^{120}\text{I}$ can be measured via the activation technique since in both cases the products are radioactive and have appropriate β -decay half-lives. In the case of $^{120}\text{Te}(p, n)^{120}\text{I}$, the product ^{120}I has ground (^{120g}I) and isomeric states (^{120m}I), and their partial cross sections can be determined separately because of the different decay pattern of the two states. The decay parameters used for this analysis are summarized in Table I. The details of the experiment are given in Sec. II.

The $^{120}\text{Te}(p, \gamma)^{121}\text{I}$ and $^{120}\text{Te}(p, n)^{120}\text{I}$ activation measurements have been performed up to 7.93 MeV as a test of the statistical model predictions over a broader energy region. The experimental cross sections have been compared with the predictions of Hauser-Feshbach statistical model calculations using the codes standard NON-SMOKER and TALYS with

TABLE I: Decay parameters of the $^{120}\text{Te} + p$ reaction products [38] and measured photo-peak efficiencies of the γ transitions, used for the analysis.

Reaction	Product	Half-life	γ Energy (keV)	γ Intensity (%)	Detection efficiency (%)
$^{120}\text{Te}(p,\gamma)$	^{121}I	(2.12 ± 0.01) h	532.08	6.1 ± 0.3	12.6 ± 0.3
$^{120}\text{Te}(p,n)$	^{120g}I	(81.6 ± 0.2) min	1523.0	10.9 ± 0.6	5.3 ± 0.1
	^{120m}I	(53 ± 4) min	654.5	2.1 ± 0.7	10.6 ± 0.2

various combinations of the nuclear inputs. This analysis is discussed in Sec. III. A summary and conclusions are provided in Sec. IV.

II. MEASUREMENTS

A. Target properties

Targets were prepared at Argonne National Laboratory and at the University of Notre Dame. 99.4% enriched ^{120}Te oxide was evaporated onto $20 \mu\text{g cm}^{-2}$ C backing [32] and 1.5 mg cm^{-2} Al backing, and two targets were produced with thicknesses of $128 \mu\text{g cm}^{-2}$ and $456 \mu\text{g cm}^{-2}$, respectively. Target frames were made of Ta, with 1 cm diameter holes. Target thicknesses were checked by Rutherford backscattering (RBS) and verified to within 9% uncertainty.

Backscattered protons were measured in order to monitor the target performance during each irradiation. For this purpose, a Si surface barrier detector with a reduced entrance aperture of 0.5 mm diameter was mounted at an angle of 135° with respect to the beam direction as shown in Fig. 1.

B. Irradiations

Activation measurements of the $^{120}\text{Te}(p,\gamma)^{121}\text{I}$ and $^{120}\text{Te}(p,n)^{120}\text{I}$ cross sections were performed at the University of Notre Dame (Indiana, USA) Tandem Van de Graaff accelerator. The accelerator provided a proton beam with energies ranging from 2.5 to

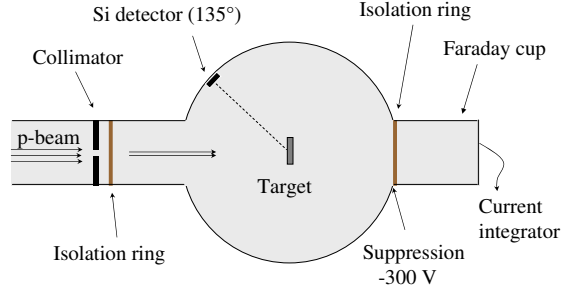


FIG. 1: A drawing of the components used in the beam line during the irradiation. The beam was defined by a upstream collimator with a diameter of 10 mm and a smaller collimator with 5 mm diameter at target position. The Si detector was placed at 135° with respect to beam direction for RBS measurements.

8.0 MeV, in steps of 0.5 MeV, in the laboratory frame. These energies correspond to effective center-of-mass energies between 2.47 and 7.93 MeV. The effective center-of-mass energies ($E_{c.m.}^{eff}$) are the proton center-of-mass energies at which one half of the reaction yield for the entire target thickness is obtained [33, 34]. This energy range covers the Gamow window for the $^{120}\text{Te}(p,\gamma)^{121}\text{I}$ reaction at a temperature of 3×10^9 K. A schematic diagram of the target irradiation chamber, located at the end of the beam line, is illustrated in Fig. 1. The incident beam current was measured with a Faraday cup mounted directly after the target chamber, and isolated from the entire beam line. A secondary electron suppression voltage of -300 V was applied at the entrance of the Faraday cup. The beam was defined by an upstream collimator with a diameter of 10 mm and a smaller collimator with 5 mm diameter at the target position mounted on a moveable target holder with two positions; one for the collimator and the other for the target. The beam was tuned by minimizing the current on both collimators and using a quartz viewer at the end of the beam line.

The stability of the beam current was monitored with an integrator in time intervals of 1 s. Since the irradiation time period was divided into segments that were sufficiently small, the beam intensity was assumed constant over each segment. The calculation of the number of reaction products in any time segment is discussed in Refs. [21, 23]. The applied current was between 80 and 320 nA, based on the thickness of the targets and beam energy. The target was irradiated for 6 h for the lowest beam energy, 2.5 MeV. With the increase of beam energy, the irradiation time decreased, with a minimum time of 15 min, because of

increasing cross section with energy.

After each irradiation, the target was removed from the target chamber and then transported to the off-line gamma counting system in order to measure the yield of the characteristic γ activity of the produced unstable isotopes, ^{121}I and ^{120}I .

C. Determination of the activity

The counting system was similar to that used previously to measure the α captures of ^{112}Sn [7] and ^{106}Cd [8]. The γ detection setup was composed of two Clover detectors placed face-to-face in close geometry, 4.9 mm apart. In order to reduce the X-rays from the decays, a 0.59 mm thick Cu plate was placed in front of each Clover, so that more than 99% of the 50 keV X-rays were suppressed. The whole assembly was shielded against room background with 5 cm of Pb and an inner 3 mm Cu lining.

The irradiated target was placed in a plexiglass holder, and then inserted into the fixed 4.9 mm gap between the Clovers in order to firmly constrain the center of the detection system for reproducibility of the detection geometry. The γ counting for each run lasted between 1 and 7 h, based on the counting statistics. Each of the crystals were counted individually (the so-called direct mode) in order to decrease pileup and summing [35]. The energies of the crystals were recorded event by event together with the time of the event. A pulser with a frequency 100 Hz was fed into one of the Ge preamplifiers, so that the dead time could be reconstructed as a function of time. Dead time corrections were performed by dividing the decay into sufficiently small time intervals depending on the count rates.

In such a close geometry, which covers a solid angle of nearly 4π , the detection efficiency is relatively high, hence the correction for coincidence summing effects becomes important. Summing correction factors (between 2% and 14%) were determined by means of summing coefficients modified from Ref. [36].

The photo-peak efficiency of the detection system was measured by the efficiency-ratio method, which is described in Refs. [7] and [37]. The relative efficiencies were obtained with an uncalibrated ^{152}Eu source (with respect to the 245 keV line γ efficiency), and normalized to the absolute photo-peak efficiency of a calibrated ^{137}Cs source. In previous works [7, 8], the coincidence method was also used and found to be in agreement with the efficiency-ratio method within the uncertainties. The nearly 4π detection geometry allowed the angular

correlation to be neglected. The absolute photo-peak efficiencies of the γ transitions used for the products of the investigated reactions, $^{120}\text{Te}(p,\gamma)^{121}\text{I}$ and $^{120}\text{Te}(p,n)^{120}\text{I}$, are given in Table I.

In order to confirm that the analysis of the γ transitions of interest is realistic, the γ peaks are confirmed not only by their energy values but also by their known decay lifetimes. The decays of the reaction products were plotted against time, and their semi-logarithmic graphs are linear within the uncertainties. This technique confirms that the analyzed γ rays are correctly identified and are associated with the isotopes of interest. As an example, a decay of ^{120}I counted for 110 min with 10 min intervals following a 22 min irradiation of ^{120}Te with 6.44 MeV protons is shown in Fig. 2. The ^{120g}I decay curve through the 1523 keV line gives a half-life of (81.3 ± 1.5) min, which is confirmed by the value taken from the literature (Table I).

III. RESULTS AND DISCUSSION

The $^{120}\text{Te}(p,\gamma)^{121}\text{I}$ and $^{120}\text{Te}(p,n)^{120}\text{I}$ cross sections have been measured in the effective center-of-mass energies between 2.47 and 7.93 MeV in order to test the consistency of statistical model cross section predictions for p -process nucleosynthesis simulations. The

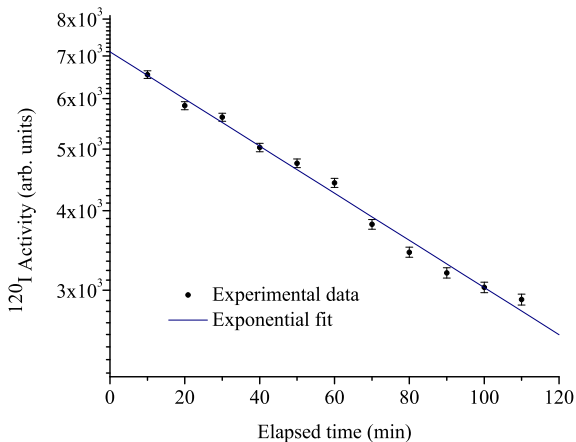


FIG. 2: Decay of ^{120g}I counted for 110 min with 10 min intervals after 22 min irradiation of ^{120}Te at a proton beam energy of 6.44 MeV. The solid line is the exponential fit to the measurement ($\chi^2 = 0.99$).

astrophysical S factors have also been determined from the measured cross sections. The experimental energy range covers the Gamow window (2.43 to 4.64 MeV at 3×10^9 K). The results for the $^{120}\text{Te}(p,\gamma)^{121}\text{I}$ and $^{120}\text{Te}(p,n)^{120}\text{I}$ reactions are summarized in Tables II and III, respectively.

The uncertainty in the results stems from the following partial errors: target thickness ($\sim 9\%$), counting statistics (0.2% to 11%), detection efficiency (1.9% to 2.4%), decay parameters (0.2% to 33%), and beam current normalization (less than 2%). The uncertainties in the effective center-of-mass energies range between 0.02% and 0.5%; they were calculated with the SRIM code [39] based on the proton energy loss in the targets. To test for systematic uncertainties, the $^{120}\text{Te}(p,\gamma)^{121}\text{I}$ reaction cross section was measured at 3.5 and 5.0 MeV using both targets whose results are in excellent agreement (Table II).

The $^{120}\text{Te}(p,n)^{120}\text{I}$ reaction produces ground (^{120g}I) and isomeric (^{120m}I) states of ^{120}I with the half-lives 81.6 min and 53 min, respectively. The cross section of this reaction was determined by summing the partial cross sections of the $^{120}\text{Te}(p,n)^{120g}\text{I}$ and $^{120}\text{Te}(p,n)^{120m}\text{I}$ reactions. The partial cross sections of these (p,n) reactions were measured by using the individual decay parameters (Table I) of the ground and isomeric states. For the analysis of (p,n) data, the 1523 keV (^{120g}I) and 654.5 keV (^{120m}I) γ transitions were chosen because these two γ transitions are associated exclusively with the decay of ground and isomeric states. The cross sections of these two (p,n) reactions are listed separately in the Table IV.

The measured cross sections and astrophysical S factors of the $^{120}\text{Te}(p,\gamma)^{121}\text{I}$ and $^{120}\text{Te}(p,n)^{120}\text{I}$ reactions have been compared with the Hauser-Feshbach statistical model calculations obtained with the standard settings of the statistical model code NON-SMOKER [30, 40] and TALYS [41] with the default parameters [42, 43, 44] (and also with parameters similar to those of the standard settings of the NON-SMOKER [26, 45, 46], as discussed later). The default optical model potentials used in TALYS are the local and global parameterizations for protons from Ref. [42]. For the nuclear level density, the TALYS code uses the parametrization by Refs. [43] and [44]. For the standard settings of the statistical code NON-SMOKER, the optical potential is the widely-used semimicroscopic potential of Jeukenne *et al.* [45] (JLM) with the low energy modifications by [46] and the nuclear level densities of Rauscher *et al.* [26].

Figure 3 shows that good agreement is generally observed for the $^{120}\text{Te}(p,\gamma)^{121}\text{I}$ cross section values, although it seems the theoretical calculations using the standard

NON-SMOKER and TALYS codes deviate considerably from the data at energies above the neutron threshold. The fact that the NON-SMOKER code underestimates the (p, n) measurements may explain why NON-SMOKER predictions overestimate the (p, γ) data at energies above 6.44 MeV. The predicted S factor values overestimate the data by approximately a factor of 2.5 above 6.44 MeV while they deviate from the experimental values by factors of less than 1.7 at energies below 6.44 MeV, for both standard codes, as seen in Fig. 4. Three points in the (p, γ) data at energies between 3.96 and 4.95 MeV are lower by a factor of 1.3 to 1.7 compared to the predictions (Fig. 4). That is well within the uncertainty range defined by the standard input parameters for the Hauser-Feshbach models. Similar behavior is seen in some (p, γ) measurements whose references are listed in

TABLE II: Measured cross sections and S factors of the $^{120}\text{Te}(p, \gamma)^{121}\text{I}$ reaction.

E_{beam} (MeV)	$E_{\text{c.m.}}^{\text{eff}}$ (MeV)	Cross section (mb)		S factor (10^{11} keV b)	
2.500	2.467±0.013	0.0023 ±	0.0003	7.62 ±	1.08
3.000	2.963±0.012	0.030 ±	0.003	7.15 ±	0.73
3.500	3.460±0.011	0.194 ±	0.019	5.91 ±	0.58
3.500	3.468±0.003	0.200 ±	0.020	6.01 ±	0.51
4.000	3.958±0.010	0.706 ±	0.069	4.16 ±	0.41
4.500	4.454±0.009	2.55 ±	0.25	3.89 ±	0.38
5.000	4.950±0.008	5.68 ±	0.56	2.77 ±	0.27
5.000	4.956±0.003	5.63 ±	0.55	2.75 ±	0.22
5.500	5.452±0.002	18.7 ±	1.8	3.43 ±	0.34
6.000	5.942±0.008	34.3 ±	3.3	2.71 ±	0.27
6.500	6.444±0.002	46.5 ±	4.5	1.74 ±	0.17
7.000	6.940±0.002	23.2 ±	2.3	0.45 ±	0.04
7.500	7.436±0.002	21.8 ±	2.2	0.24 ±	0.02
8.000	7.932±0.002	16.5 ±	1.7	0.10 ±	0.01

TABLE III: Measured cross sections and S factors of the $^{120}\text{Te}(p, n)^{120}\text{I}$ reaction.

E_{beam}	$E_{\text{c.m.}}^{\text{eff}}$	Cross section		S factor	
(MeV)	(MeV)	(mb)		(10^{11} keV b)	
6.500	6.444±0.002	20.6 ±	2.1	0.77 ±	0.08
7.000	6.940±0.002	72.6 ±	7.5	1.41 ±	0.14
7.500	7.436±0.002	133 ±	13	1.44 ±	0.14
8.000	7.932±0.002	178 ±	18	1.12 ±	0.11

 TABLE IV: Measured cross sections of the $^{120}\text{Te}(p, n)^{120}\text{I}$ reactions that produce ground ^{120g}I and isomeric ^{120m}I states. For the analysis, 1523 keV and 654.5 keV γ transitions, respectively, were used: for the decay parameters see Table I.

E_{beam}	$E_{\text{c.m.}}^{\text{eff}}$	Cross Section (mb)	
(MeV)	(MeV)	^{120g}I (1523 keV)	^{120m}I (654.5 keV)
6.500	6.444±0.002	19.1±2.0	1.53±0.66
7.000	6.940±0.002	65.4±6.8	7.2±3.0
7.500	7.436±0.002	123±13	10.8±4.5
8.000	7.932±0.002	160±16	18.1±7.5

the Sec. I, especially for the $^{86}\text{Sr}(p, \gamma)^{87}\text{Y}$ reaction [12].

For the $^{120}\text{Te}(p, \gamma)^{121}\text{I}$ reaction, the energy dependence of the astrophysical S factor is slightly better described by the statistical model code TALYS with the default parameters at energies below 6.94 MeV (Fig. 4). The difference between the predictions of the two model codes can mainly be attributed to the different proton optical potential and nuclear level densities used in the codes. In order to try and identify the source of the observed discrepancies between the two calculations, the optical model potentials (OMP) and nuclear level densities (NLD) of TALYS were varied. Various combinations of the nuclear parameters, and their labels, used in the model codes are given in Table V.

The impact of different parameters (as indicated with TALYS-BSFG-JLM for the TALYS S factor predictions) is shown in Fig. 4 compared to the predictions of NON-SMOKER for its

TABLE V: Model calculations using TALYS and NON-SMOKER codes with various combinations of the nuclear parameters: nuclear level densities (NLD), and optical model parameters (OMP). JLM model used in TALYS and NON-SMOKER is with the modification of [47] and [46], respectively.

Label	NLD-model	OMP
TALYS-BSFG-JLM	BSFG [41]	JLM [45, 47]
TALYS-CTFG-JLM	CTFG [41]	JLM [45, 47]
TALYS-BSFG-KD	BSFG [41]	KD [42]
TALYS-default	CTFG [41]	KD [42]
NON-SMOKER-standard	BSFG [40]	JLM [45, 46]

standard settings. The experimental $^{120}\text{Te}(p,\gamma)^{121}\text{I}$ S factor results are within the uncertainty range resulting from the choice of different parameter settings. Figure 4 also shows that the predictions of both TALYS and NON-SMOKER using similar parameters (standard NON-SMOKER) have the same energy dependence. However, TALYS-BSFG-JLM is generally lower than the standard NON-SMOKER prediction by a factor of 2. In order to investigate which parameters cause the changes in magnitude, only one parameter of

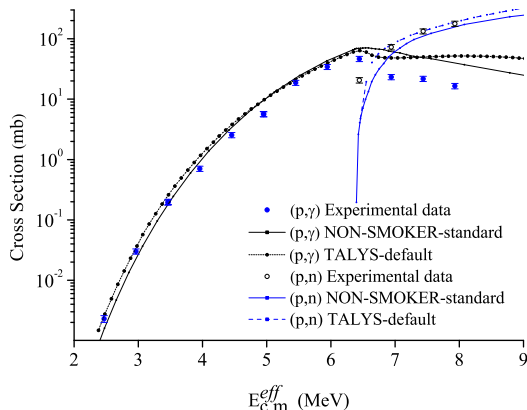


FIG. 3: (Color online) The experimental cross section results of $^{120}\text{Te}(p,\gamma)^{121}\text{I}$ and $^{120}\text{Te}(p,n)^{120}\text{I}$ reactions in comparison with standard NON-SMOKER [40] and TALYS predictions with the default parameters [41].

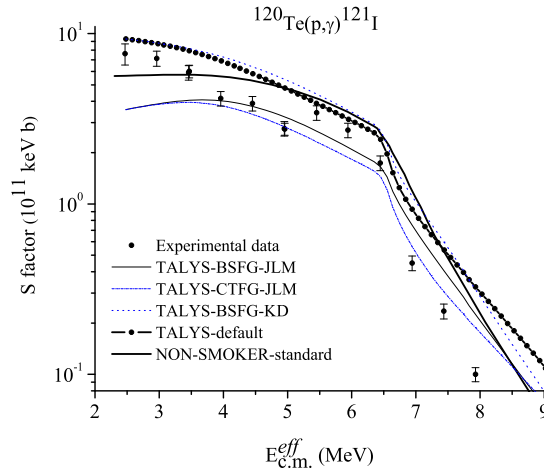


FIG. 4: (Color online) Comparison of predicted astrophysical S factors of $^{120}\text{Te}(p,\gamma)^{121}\text{I}$ reaction with four different TALYS code calculations, and standard NON-SMOKER code, using the combinations of nuclear parameters described in Table V. The experimental S factors of the (p,γ) reaction are also presented. The JLM model used in TALYS and NON-SMOKER is with the modification of [47] and [46], respectively.

the default TALYS was changed each time. The changes in the OMP and NLD are labeled TALYS-CTFG-JLM and TALYS-BSFG-KD, respectively, in Fig. 4. The results indicate that the OMP is the most critical parameter for the setting of magnitude. Indeed, TALYS uses the optical nucleon potential of Jeukenne *et al.* [45] (with the modification of Bauge *et al.* [47]) without the low-energy modifications, unlike the standard NON-SMOKER (low energy modifications by [46]). It should be also emphasized that both codes apply the constant temperature formula [44] for the nuclear level density in order to correct the behavior due to the divergence of the Fermi-gas model at very low excitation energies. As the energy increases, the results of TALYS-BSFG-KD predictions deviate from the ones using TALYS with its standard default parameters and shows a similar energy dependence as compared to the standard NON-SMOKER predictions.

In the case of the $^{120}\text{Te}(p,n)^{120}\text{I}$ reaction, a better agreement is found between the experimental data and both standard codes (Figs. 3 and 5). The NON-SMOKER calculations of the astrophysical S factors underestimate the measured values by factors less than 1.4 while the TALYS predictions and the data for the studied energies are in excellent agreement, with the exception of the point at 6.44 MeV, as seen in Fig. 5. The

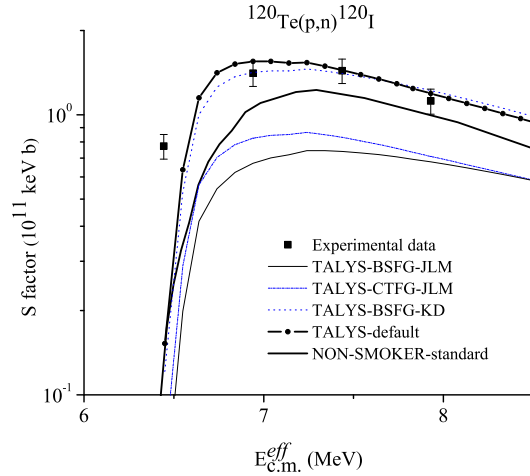


FIG. 5: (Color online) Comparison of predicted astrophysical S factors of $^{120}\text{Te}(p,n)^{120}\text{I}$ reaction with four different TALYS code calculations, and standard NON-SMOKER code, using the combinations of nuclear parameters described in Table V. The experimental S factors of the (p,n) reaction are also presented. The JLM model used in TALYS and NON-SMOKER is with the modification of [47] and [46], respectively.

predicted S factor of NON-SMOKER and TALYS at this particular energy are below the experimental value by a factor of 5. The (p,n) channel opens around this energy (Q -value of 6.397 MeV corresponding to the threshold value of 6.451 MeV). The fact that the codes use the experimentally known Q -value with 20 keV uncertainty could explain, in part, the difference at the lowest measured energy for the (p,n) reaction because the cross section decreases steeply at energies near the threshold value.

The same variations in the nuclear parameters (Table V) of the code TALYS were applied to the (p,n) reaction. Figure 5 shows that the S factor results of NON-SMOKER provide better agreement with the experimental data than those of TALYS when the standard NON-SMOKER parameters are used (as indicated with TALYS-BSFG-JLM). The model calculations are more sensitive to the choice of OMP than the other nuclear parameters, as seen in Fig. 5.

IV. SUMMARY AND CONCLUSIONS

The total cross sections of the reactions $^{120}\text{Te}(p,\gamma)^{121}\text{I}$ and $^{120}\text{Te}(p,n)^{120}\text{I}$ have been measured via the activation method, and their astrophysical S factors have been derived in the effective center-of-mass energy range between 2.47 and 7.93 MeV.

Measurements of the cross sections were performed for a broad energy range, covering the Gamow window centered at 3.53 MeV for $T = 3 \times 10^9$ K. It has been pointed out that in cases where a nuclear reaction proceeds through narrow resonances, an effective stellar energy window can differ significantly from the commonly used Gamow peak [48]. However, for heavier nuclei, the nuclear level density is high, and the cross section is characterized by a multitude of overlapping resonances which is eligible for the statistical Hauser-Feshbach treatment [26].

The experimental results of astrophysical S factors for the $^{120}\text{Te}(p,\gamma)^{121}\text{I}$ and $^{120}\text{Te}(p,n)^{120}\text{I}$ reactions have been compared with the predictions of statistical model calculations using the standard NON-SMOKER code as well as the TALYS code with various combinations of the nuclear parameters (listed in Table V). The discrepancies in the results between the predictions are relatively small and can be attributed to the choice of nuclear input parameters used in the codes. The S factor results are more sensitive to the OMP than to the NLD in the astrophysically relevant low-energy region, for both (p,γ) and (p,n) reactions. The best overall agreement is obtained with the OMPs of KD [42] using the code TALYS.

For the $^{120}\text{Te}(p,\gamma)^{121}\text{I}$ reaction, the default setting of TALYS (-CTFG-KD) offers a better reproduction below the (p,n) threshold. Changing the OMP of TALYS to JLM [45] gives a poor reproduction as a whole. The deviations at the very lowest energies are expected because OMP is parameterized as a function of energy over a broader mass region [11]. It should be also emphasized that the (p,γ) S factors are very sensitive to the proton width at the lowest energies [10, 22].

In the case of the $^{120}\text{Te}(p,n)^{120}\text{I}$ reaction, the code TALYS with the default parameters is able to reproduce the data very well except for the point at 6.44 MeV. This has been identified as a threshold effect. The choice of OMPs clearly plays a critical role over the entire energy region. It should be emphasized that (p,n) reactions are also sensitive to the proton width at all energies [10, 22].

Overall, the results of the experiments indicate good agreement with the theoretical predictions within the uncertainty range of the nuclear structure input parameters for the model predictions. This confirms earlier observations of p -process reaction measurements on lower Z targets and confirms the validity of Hauser-Feshbach model applications for p -process reactions over the entire mass range from $Z=35$ to $Z=52$. The results for the specific proton capture reaction on ^{120}Te suggests that the Hauser-Feshbach predictions for the inverse stellar photo disintegration process [31] are also reliable within the model uncertainty range.

Acknowledgments

This work was supported by The Scientific and Technological Research Council of Turkey TUBITAK-Grant-108T508, Kocaeli University BAP- Grant-2007/36, the National Science Foundation NSF-Grant-0434844, the Joint Institute for Nuclear Astrophysics JINA (www.JINAweb.org) PHY02-16783, and The Hungarian Scientific Research Fund Programs OTKA (K68801, T49245).

-
- [1] S. E. Woosley and W. M. Howard, *Ap. J. Suppl.* **36**, 285 (1978).
 - [2] M. Rayet, N. Prantzos, and M. Arnould, *Astron. Astrophys.* **227**, 271 (1990).
 - [3] W. Rapp, J. Görres, M. Wiescher, H. Schatz, and F. Käppeler, *Astrophys. J.* **653**, 474 (2006).
 - [4] M. Rayet, M. Arnould, M. Hashimoto, N. Prantzos, and K. Nomoto, *Astron. Astrophys.* **298**, 517 (1995).
 - [5] M. Arnould and S. Goriely, *Phys. rep.* **384**, 1 (2003).
 - [6] E. Somorjai, Zs. Fülöp, A. Z. Kiss, C. Rolfs, HP. Trautvetter, U. Greife, M. Junker, S. Goriely, M. Arnould, M. Rayet, T. Rauscher, and H. Oberhummer, *Astron. Astrophys.* **333**, 1112 (1998).
 - [7] N. Özkan, G. Efe, R. T. Güray, A. Palumbo, J. Görres, H. -Y. Lee, L. O. Lamm, W. Rapp, E. Stech, M. Wiescher, G. Gyürky, Zs. Fülöp, E. Somorjai, *Phys. Rev. C* **75**, 025801 (2007).
 - [8] Gy. Gyürky, G. G. Kiss, Z. Elekes, Zs. Fülöp, E. Somorjai, A. Palumbo, J. Görres, H. Y. Lee, W. Rapp, M. Wiescher, N. Özkan, R. T. Güray, G. Efe, and T. Rauscher, *Phys. Rev. C* **74**, 025805 (2006).

- [9] C. Yalçın, R. T. Güray, N. Özkan, S. Kutlu, Gy. Gyürky, J. Farkas, G. G. Kiss, Zs. Fülöp, A. Simon, E. Somorjai, and T. Rauscher, *Phys. Rev. C* **79**, 065801 (2009).
- [10] G. G. Kiss, Gy. Gyürky, Z. Elekes, Zs. Fülöp, E. Somorjai, T. Rauscher, M. Wiescher, *Phys. Rev. C* **76**, 055807 (2007).
- [11] Gy. Gyürky, Zs. Fülöp, E. Somorjai, M. Kokkoris, S. Galanopoulos, P. Demetriou, S. Harissopulos, T. Rauscher, and S. Goriely, *Phys. Rev. C* **68**, 055803 (2003).
- [12] Gy. Gyürky, E. Somorjai, Zs. Fülöp, S. Harissopulos, P. Demetriou, and T. Rauscher, *Phys. Rev. C* **64**, 065803 (2001).
- [13] S. Galanopoulos, P. Demetriou, M. Kokkoris, S. Harissopulos, R. Kunz, M. Fey, J. W. Hammer, Gy. Gyürky, Zs. Fülöp, E. Somorjai, and S. Goriely, *Phys. Rev. C* **67**, 015801 (2003).
- [14] P. Tsagari, M. Kokkoris, E. Skreti, A. G. Karydas, S. Harissopulos, T. Paradellis, and P. Demetriou, *Phys. Rev. C* **70**, 015802 (2004).
- [15] C. E. Laird, D. Flynn, R. L. Hershberger, and F. Gabbard, *Phys. Rev. C* **35**, 1265 (1987).
- [16] S. Harissopulos, E. Skreti, P. Tsagari, G. Souliotis, P. Demetriou, T. Paradellis, J. W. Hammer, R. Kunz, C. Angulo, S. Goriely, and T. Rauscher, *Phys. Rev. C* **64**, 055804 (2001).
- [17] T. Sauter and F. Kämpeler, *Phys. Rev. C* **55**, 3127 (1997).
- [18] F. R. Chloupek, A. St. J. Murphy, R. N. Boyd, A. L. Cole, J. Görres, R. T. Güray, G. Raimann, J. J. Zack, T. Rauscher, J. V. Schwarzenberg, P. Tischhauser, and M. Wiescher, *Nucl. Phys.* **A652**, 391 (1999).
- [19] J. Bork, H. Schatz, F. Kämpeler, and T. Rauscher, *Phys. Rev. C* **58**, 524 (1998).
- [20] N. Özkan, A. St. J. Murphy, R. N. Boyd, A. L. Cole, R. deHaan, M. Famiano, J. Görres, R. T. Güray, M. Howard, L. Sahin, and M. Wiescher, *Nucl. Phys.* **A688**, 459c (2001).
- [21] N. Özkan, A. St. J. Murphy, R. N. Boyd, A. L. Cole, M. Famiano, R. T. Güray, M. Howard, L. Sahin, J. J. Zack, R. deHaan, J. Görres, M. C. Wiescher, M. S. Islam, and T. Rauscher, *Nucl. Phys.* **A710**, 469 (2002).
- [22] Gy. Gyürky, G. G. Kiss, Z. Elekes, Zs. Fülöp, E. Somorjai, and T. Rauscher, *J. Phys. G: Nucl. Part. Phys.* **34**, 817 (2007).
- [23] M. A. Famiano, R. S. Kodikara, B. M. Giacheri, V. G. Subramanian, A. Kayani, *Nucl. Phys.* **A802**, 26-44 (2008).
- [24] G. G. Kiss, T. Rauscher, Gy. Gyürky, A. Simon, Zs. Fülöp, and E. Somorjai, *Phys. Rev.*

- Letters 101, 191101 (2008).
- [25] A. Spyrou, A. Lagoyannis, P. Demetriou, S. Harissopulos, and H.-W. Becker, Phys. Rev. C **77**, 065801 (2008).
- [26] T. Rauscher, F.-K. Thielemann, and K.-L. Kratz, Phys. Rev. C **56**, 1613 (1997).
- [27] T. Rauscher, Phys. Rev. C **73**, 015804 (2006).
- [28] H. Utsunomiya, P. Mohr, A. Zilges, and M. Rayet, Nucl. Phys. **A777**, 459 (2006).
- [29] P. Mohr, Zs. Fülöp, H. Utsunomiya, Eur. Phys. J. A **32**, 357 (2007).
- [30] T. Rauscher and F.-K. Thielemann, At. Data Nucl. Data Tables **75**, 1 (2000).
- [31] T. Rauscher and F.-K. Thielemann, At. Data Nucl. Data Tables **88**, 1 (2004).
- [32] J. Greene, A. Palumbo, W. Tan, J. Görres, M. C. Wiescher, Nucl. Instr.: Meth. In Phys. Res. A **590**, 76-78 (2008).
- [33] C. Iliadis, *Nuclear Physics in Stars* (Wiley-VCH, Berlin, 2007).
- [34] C. E. Rolfs and W. S. Rodney, *Cauldrons in the Cosmos* (University of Chicago Press, Chicago, 1988).
- [35] S. Dababneh, N. Patronis, P. A. Assimakopoulos, J. Görres, M. Heil, F. Käppeler, D. Karamanis, S. O'Brien, and R. Reifarth, Nucl. Instr. and Meth. A **517**, 230 (2004).
- [36] F. J. Shima and D. D. Hoppea, Int. J. Appl. Radiat. Isotopes **38**, 1109 (1983).
- [37] K. Debertin and R.G. Helmer, *Gamma-And X-ray Spectrometry With Semiconductor Detectors* (North-Holland, Amsterdam, 1989).
- [38] <http://www.nndc.bnl.gov/nudat2/>
- [39] J. P. Biersacke and J. F. Ziegler, SRIM code Version SRIM-2008.04.
- [40] T. Rauscher and F. K. Thielemann, At. Data Nucl. Data Tables **79**, 47 (2001).
<http://nucastro.org/reaclib.html>.
- [41] A. Koning, S. Hilaire, M. C. Duijvestijn, TALYS: Comprehensive nuclear reaction modeling, Proceedings of the International Conference on Nuclear Data for Science and Technology - ND2004, AIP vol. 769, eds. R.C. Haight, M.B. Chadwick, T. Kawano, P. Talou, Sep. 26 - Oct. 1, 2004, Santa Fe, USA, p. 1154 (2005). <http://www.talys.eu>
- [42] A. J. Koning and J. P. Delarache, Nucl. Phys. **A713**, 231 (2003).
- [43] T. Ericson, Adv. Phys. **9**, 425 (1960).
- [44] A. Gilbert and A. G. W. Cameron, Can. J. Phys. **43**, 1446 (1965).
- [45] J. P. Jeukenne, A. Lejeune, and C. Mahaux, Phys. Rev. C **16**, 80 (1977).

- [46] A. Lejeune, Phys. Rev. C **21**, 1107 (1980).
- [47] E. Bauge, J. P. Delaroche, and M. Girod, Phys. Rev. C **63**, 024607 (2001).
- [48] J. R. Newton, C. Iliadis, A. E. Champagne, A. Coc, Y. Parpottas, and C. Ugalde, Phys. Rev. C **75**, 045801 (2007).